Preprints of the 19th World Congress
The International Federation of Automatic Control
Cape Town, South Africa. August 24-29, 2014

LED path recovery in a moving sensor

Dongfang Zheng * **Gang Chen** * **Jay A. Farrell** *

* *Department of Electrical Engineering, University of California Riverside, Riverside, CA, 92521, USA (e-mail: (dzheng,gachen,farrell)@ee.ucr.edu)*

Abstract: Existing Visible Light Communication (VLC) methods can recover each LED's on-off status only after its projection location is identified on each image. Identifying the LED projection is challenging because: 1) Clutter and noise corrupt the measurements; 2) The LED status will be "off" in some frames; 3) The predicted projection location sequence depends on the estimated vehicle state trajectory, which is uncertain. This article presents a new method determining the q most probable data and LED position sequences simultaneously, using Bayesian multiple hypothesis tracking (MHT) techniques by maximizing posterior probabilities. This article focuses on the VLC data and LED position sequence extraction, that includes vehicle state estimation. The MHT based algorithm is demonstrated by the simulation results.

Keywords: Navigation, Data association, Multiple hypotheses tracking.

1. INTRODUCTION

LED illumination sources have long operational life, low power consumption, and are mechanically robust, leading to their growing popularity. The multifunctional capabilities of LED's are attracting increasing attention. For example, their fast switching rates ($> 100MHz$) enables LED's installed for illumination to also be used for communication and positioning, see Kavehrad (2007). Communication systems using LED's and either cameras or linear arrays have been introduced in Nagura et al. (2010); Liu et al. (2011); Arai et al. (2008); Zheng et al. (2013a).

A VLC imaging array (camera or linear) collects all the light incident on its active element, including both the signal and background light, which after processing provides a data stream including the LED ID. The LED data is modulated using as on-off keying (OOK) scheme. Recovering the LED data requires extracting the "on" and "off" sequence of the LED from a record of consecutive scans. A camera traversing a region with blinking LED acquires a sequence of images, each potentially containing a high intensity set of pixels for each on LED. Camera motion causes each LED's projected position to move across the imaging array. Extraction of the data requires this projected LED trajectory and flashing sequence to be extracted. Fig. 1 depicts two such LED trajectories and data sequences as might be extracted from an image sequence.

The challenge in this process is to accurately predict the LED location in each image, because the navigation state is uncertain. For each LED and each image, based on the navigation state and uncertainty estimates, a likely detection region can be computed and searched. However, due to the clutter and noise, multiple potential measurements may appear in this search region. This can be the case even when the LED is off. Multiple detections results in a multiple hypothesis data association problem, see Elfring et al. (2010). If a false measurement is associated

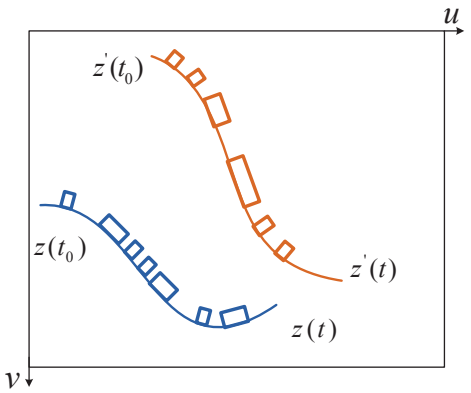

Fig. 1. Two LED trajectories and data sequences illustrated on an image plane

to the LED, then incorrect data or ID may be recovered so that the navigation state will not be updated. If this happens for several time steps, poor state estimates may result, causing the search area to grow, which exacerbates the data association challenges. It could be even worse when a correct ID is recovered, as it would associate a false measurement to the identified LED. Trusting a false measurement could cause incorrect state estimation.

When multiple detections exist within the search area, the data association problem could be solved by choosing the measurement that is closest to the predicted measurement position in Mahalanobis sense, see Maesschalck et al. (2000). This method does not work in this application, among other issues, it fails in the presence of noise or clutter when the LED is off. Another method that accounts for the null hypothesis (the LED is off) can be implemented using the probabilistic data association filter, as in Bar-Shalom et al. (2009). Though this method works in theory, there is a very low probability to obtain a correct data sequence when it is long. A Viterbi based algorithm is proposed in Zheng et al. (2014) for a linear array when

the sensor is stationary or moving with a bandwidth that is low relative to the imaging rate. Even though the LED switching frequency can be modulated up to hundreds of megahertz, sometimes we still prefer to utilize a low rate sensor (i.e., 30Hz) such as a webcam or a cellphone camera to receive the data using undersampling methods Robert (2013). In such a case, the low rover bandwidth assumption for the algorithm in Zheng et al. (2014) is not valid.

More sophistic methods can be developed using MHT methods, see Reid (1979); Bar-Shalom et al. (2005); Kurien (1990). MHT uses a deferred-decision approach in which they maintain the complete set of possible data associations within a sliding window, putting off hard decisions as long as possible, see Frank et al. (2012). Decisions are made by evaluating the probabilities of each sequence of data association hypotheses. Since the number of possible sequences increases exponentially, it is expensive to keep all of them. It is also inefficient to compute the probabilities of all possible sequences and then discarding most of them. To solve these problems, an efficient Hypothesis Oriented MHT (HOMHT) was firstly proposed in Cox and Hingorani (1996). The basic idea of this method is to keep only the q best sequences, discarding the other sequences that have low probability.

In this paper, we reformulate the LED ID recovery problem as a HOMHT problem to improve the probability of obtaining the correct ID in a computationally efficient manner. The solution to this problem provides both the data sequence and the sequence of LED projection locations on the image. This information is useful for the vehicle state trajectory estimation.

This paper is organized as follows: Section 2 defines the predicted region and data association hypothesis, and formulates the problem mathematically. Section 3.1 analyzes the posterior probability of the joint hypothesis. Section 3.2 introduces the implement method obtaining q-best hypotheses. Section 4 shows the experimental results.

2. PROBLEM FORMULATION

The photo-detector is assumed to be part of a rigid system with kinematic state (i.e., position, velocity, attitude) denoted by $x(t)$. We will refer to this rigid system as a *rover*. The rover trajectory evolves over time according to

$$\dot{x} = f(x, u), \tag{1}$$

where f is a known nonlinear mapping and u is the system input. In our navigation system, the input u represents the rover's motion information, which is measured by an encoder or inertial measurement unit (IMU).

The l-th LED at location F_l projects onto the rover photo-detector at position $z_l(t) = h(x(t), F_l)$ at time t, where the projection function h is defined in Zheng et al. (2013b) (camera) and Zheng et al. (2013a) (linear array). Each LED is switching its "on" or "off" status to communicate information to the rover.

Given a time interval $\lambda \in [t_s, t]$, the projected position of the l-th LED $z_l(\lambda)$ defines a trajectory across the photo-detector. Detection of the projected LED position depends on the LED "on" or "off" status, as well as environmental conditions and interference from other light sources. The accuracy of each LED's recovered on-off status is highly dependent on the accuracy of the data association at each time step. Therefore, the data recovery and trajectory estimation problems are coupled. Improvement in the solution of either problem enhances the solution of the other.

The purpose of this article is to develop an algorithm that simultaneously estimates the most likely data association sequences and navigation system state for each time interval $\lambda \in [t_s, t]$. Without loss of generality, we define $t_s = 0$ and the total number of time steps in the interval is K.

2.1 Predicted Measurement Region

The computer calculates an estimate $\hat{x}$ of x according to $\dot{\hat{x}} = f(\hat{x}, \hat{u})$, where $\hat{u}$ is the measurement of u. Define $\delta x = x - \hat{x}$ as the state error. The value of δx at each time is unknown; however, its linearized discrete-time state transition is modeled as

$$\delta x(k) = \Phi_{k-1}\delta x(k-1) + \omega_{k-1}, \tag{2}$$

where Φ_{k-1} is the state transition matrix from time step $k-1$ to time step k, and $\omega_{k-1} \sim \mathcal{N}(0, Q_{k-1})$ is the process noise. Methods to compute Φ_{k-1} and Q_{k-1} are presented in Section 7.2.5.2 of Farrell (2008). The state covariance P_k evolves over time according to $P_k = \Phi_{k-1}P_{k-1}\Phi_{k-1}^\top + Q_{k-1}$.

Given the state estimate at time step k, it is straightforward to compute both the predicted measurement position of the l-th LED $\hat{z}_l(k)$ and its error covariance $S_l(k)$, where

$$\hat{z}_l(k) = h(\hat{x}(k), F_l), \tag{3}$$

$$S_l(k) = H_{l,k}P_kH_{l,k}^\top + R_{l,k}, \tag{4}$$

where $H_{l,k}$ is the linearized measurement matrix, and $R_{l,k}$ is the covariance of measurement noise, both of which are defined in Zheng et al. (2011). The quantities $\hat{z}_l(k)$ and $S_l(k)$ define a prior distribution for the LED trajectory that can focus the algorithm. A region in the measurement space for the l-th LED can be defined as

$$\begin{aligned} V_{l,\gamma}(k) &\triangleq \{z : (z(k) - \hat{z}_l(k))^\top S_l^{-1}(k)(z(k) - \hat{z}_l(k)) \le \gamma\} \\ &= \{z : r_l(k)^\top S_l^{-1}(k) r_l(k) \le \gamma\}, \end{aligned} \tag{5}$$

where $r_l(k) = z(k) - \hat{z}_l(k)$ is the residual and γ is a parameter that determines the probability that the real measurement falls in $V_{l,\gamma}(k)$. For the camera and linear array measurement, the region $V_{l,\gamma}$ represents the interior of an ellipse and segment, respectively. In the following, without loss of generality, we only consider a single LED in its predicted region $V_{l,\gamma}$; therefore, we drop the l subscript. The parameter γ is selected using a χ^2-distribution table. In the examples to follow, γ is selected such that the probability that the residual falls within $V_{l,\gamma}$ is 0.997.

2.2 Data Association Hypothesis

The set of measurements that fall into the predicted region $V_{l,\gamma}$ at time step k are

$$Z(k) \triangleq \{z_j(k)\}_{j=1}^{m_k}, \tag{6}$$

where $z_j(k)$ is the position of j-th detection and m_k is the total number of them. Since each or none of the measurements in this set could have originated from the LED, the number of data association hypotheses is $(m_k + 1)$. Suppose there are total of K time steps, the state estimates $\{\hat{x}(k)\}_{k=1}^{K}$ and its covariance matrix $\{P_k\}_{k=1}^{K}$ are calculated based on the inputs $U^K = \{u(k)\}_{k=1}^{K}$ and prior state distribution $x(0) \sim \mathcal{N}(\hat{x}(0), P_0)$. Then the predicted region at each time step is calculated by eqns. (3-5), and the measurements that fall into V_γ are extracted. We also define $Z^k \triangleq \{Z(j)\}_{j=1}^{k}$, as the set of measurements up to time step k. Since there are total of K time steps, the number of joint data association hypotheses is

$$L_K = \prod_{k=1}^{K}(m_k + 1). \tag{7}$$

Each data association sequence corresponds to a LED trajectory across the detector, which in turn decodes a sequence of detection and nondetection events into an ID sequence.

A symbol $\theta^{k,\ell}$, where $\ell \in [1, L_k]$, represents a specific list of joint data association hypotheses up to time step k. For example, a hypothesis $\theta^{k,\ell}$ has the form

$$\theta^{k,\ell} = \{j_1, j_2, \cdots, j_i, \cdots, j_k\}, \tag{8}$$

where $j_i \in [0, m_i]$. The symbol $\theta^{k,\ell}(i) = j$ represents that the j-th detection at time step i is originated from the LED and $\theta^{k,\ell}(i) = 0$ represents that none of the measurements at time step i is originated from the LED. We say the joint hypothesis $\theta^{k,\ell}$ is an extension of $\theta^{k-1,s}$, if $\theta^{k,\ell} = \{\theta^{k-1,s}, j_k\}$ where $j_k \in [0, m_k]$. Herein, the symbol ℓ and s in the superscribe of θ are not necessarily identical, since the two hypotheses are enumerated independently at different time steps. Note that each joint data association hypothesis includes a potentially distinct posterior vehicle trajectory.

2.3 Technical Problem Statement

Given the measurement set, we would like to find the most probable joint data association hypotheses (i.e. q-best hypotheses $\{\theta^{K,\ell}\}_{\ell=1}^{q}$). After these hypotheses are found, their corresponding ID sequences are straightforward to recover. By comparing each of the recovered ID with the predicted ID, the most probable data association hypothesis with correct ID is found and used for the navigation state update. The advantage of finding q-best hypotheses instead of only the most probable one is, several candidate hypotheses indicate more chances to recover the correct ID.

The problem is state as: Given measurements Z^K and navigation system inputs U^K, find the q-best joint data association hypotheses $\{\theta^{K,\ell}\}_{\ell=1}^{q}$ among the total number of L_K hypotheses, where q-best means the q hypotheses that maximize the hypothesis posterior probability.

3. METHOD

We firstly evaluate the posterior probability mass function (pmf) of a joint data association hypothesis up to time step k. We assume that the measurements due to clutter are uniformly distributed in the predicted region V_γ.

3.1 Hypothesis Probability

The joint probability of an association hypothesis up to time step $k \in [1, K]$ is

$$\begin{aligned} & p\left(\theta^{k,\ell} \mid Z^k, U^{k-1}\right) \\ &= \frac{1}{c} p(\theta^{k,\ell}, Z(k) \mid Z^{k-1}, U^{k-1}) \\ &= \frac{1}{c} p(Z(k) \mid \theta(k), \theta^{k-1,s}, Z^{k-1}, U^{k-1}) \cdot \\ & \quad p(\theta(k) \mid \theta^{k-1,s}, Z^{k-1}, U^{k-1}) p\left(\theta^{k-1,s} \mid Z^{k-1}, U^{k-2}\right), \end{aligned} \tag{9}$$

where the normalization factor $c = p\left(Z(k) \mid Z^{k-1}, U^{k-1}\right)$ is independent of the data association hypothesis $\theta^{k,\ell}$.

The first term in the right hand side (RHS) of eqn. (9) is the joint probability of the current measurement position distribution given the hypotheses, measurements and inputs of all the previous time steps. Since the different measurements in set $Z(k)$ are independent, it is decomposed as

$$\begin{aligned} & p(Z(k) \mid \theta^{k,\ell}, Z^{k-1}, U^{k-1}) \\ &= \prod_{j=1}^{m_k} p(z_j(k) \mid \theta^{k,\ell}, Z^{k-1}, U^{k-1}) = \prod_{j=1}^{m_k} f(j). \end{aligned} \tag{10}$$

The measurements due to clutter or false alarm are assumed to be uniformly distributed in the predicted region, while the one from LED is assumed to be corrupted by Gaussian noise. Therefore, we have

$$f(j) = \begin{cases} \dfrac{1}{V} & \text{for clutter,} \\ \mathcal{N}(z_j(k); \hat{z}^s(k), S^s(k)) & \text{for the LED,} \end{cases} \tag{11}$$

where V is the volume (area) of predicted region. The predicted measurement position and its error covariance under the hypothesis $\theta^{k-1,s}$ are represented as $\hat{z}^s(k)$ and $S^s(k)$), respectively. Note that this step includes state estimation.

The second term of eqn. (9) is the prior probability of the association hypothesis, and is given by

$$\begin{aligned} & p(\theta(k) \mid \theta^{k-1,s}, Z^{k-1}, U^{k-1}) \\ &= \begin{cases} \dfrac{1}{m_k} P_{on} \mu_F(m_k - 1) & \text{for } \theta(k) = 1 \cdots m_k, \\ (1 - P_{on}) \mu_F(m_k) & \text{for } \theta(k) = 0, \end{cases} \end{aligned} \tag{12}$$

where P_{on} is the probability that the LED is on. In eqn. (12), the number of measurements due to clutter and false alarms is modeled as a Poisson process, see Bar-Shalom et al. (2005), with distribution function μ_F parameterized by λ:

$$\mu_F(\phi) = \exp^{-\lambda V} \frac{(\lambda V)^\phi}{\phi!}. \tag{13}$$

Let $\beta^{k,\ell} = p(\theta^{k,\ell} \mid Z^k, U^{k-1})$ denote the posterior pmf of $\theta^{k,\ell}$ in eqn. (9). Substituting eqn. (10) - (13) into eqn. (9) and combining the constants into c', the probability is

$$\beta^{k,\ell} = \begin{cases} \frac{1}{c'}\mathcal{N}^{k-1,s}(z_j(k))P_{on}\beta^{k-1,s} & \text{for } \theta(k) = j \neq 0 \\ \frac{1}{c'}\lambda(1-P_{on})\beta^{k-1,s} & \text{for } \theta(k) = 0, \end{cases} \quad (14)$$

where $\mathcal{N}^{k-1,s}(z_j(k)) = \mathcal{N}(z_j(k); \hat{z}^s(k), S^s(k))$, and $c' = c \cdot e^{\lambda V} \cdot m_k! \cdot \lambda^{1-m_k}$.

From eqn. (14), the marginal likelihood function for the hypothesis that the j-th measurement at time step k has originated from the LED is

$$\mathcal{L}_{s,j}(k) = \mathcal{N}^{k-1,s}(z_j(k))P_{on}, \quad (15)$$

and the marginal likelihood function for the hypothesis that no measurement at time step k is from the LED is

$$\mathcal{L}_{s,0}(k) = \lambda(1-P_{on}). \quad (16)$$

Then the probability that hypothesis $\theta(k) = j$ is the extension of joint hypothesis $\theta^{k-1,s}$ is

$$p(\theta(k) = j \mid Z^k, \theta^{k-1,s}, U^{k-1}) = \frac{\mathcal{L}_{s,j}(k)}{\sum_{i=0}^{m_k}\mathcal{L}_{s,i}(k)}. \quad (17)$$

3.2 q-best Hypotheses

Computing the probability of all possible hypotheses and then discarding most of them is inefficient. Only those hypotheses having relatively high probability are considered to be the candidate LED paths. An efficient method to implement the hypothesis based MHT (HOMHT) was first introduced in Cox and Hingorani (1996). The basic idea of this method is to only keep the q-best hypotheses, discarding the hypotheses that have lower probability. This method employs Murty's algorithm Murty (1968) to find the j-th best hypothesis solution.

Given the q-best hypotheses $\{\theta^{k-1,i}\}_{i=1}^q$ up to the former step and their corresponding probabilities $\{\beta^{k-1,i}\}_{i=1}^q$, and the measurement set $Z(k)$, the new q-best hypotheses $\{\theta^{k,i}\}_{i=1}^q$ up to the current time step will be generated. Define $\theta^{k-1,i}$ to be the parent hypothesis of $\theta^{k,j}$, if the latter is the extension of the former. Choosing the single hypothesis j_k at time step k is the process of generating the extension of $\theta^{k-1,i}$. The best extension of $\theta^{k-1,i}$ is defined as $\theta^{k,i_1} = \{\theta^{k-1,i}, j_k\}$ where $j_k = \arg\max_j \mathcal{L}_{i,j}$. The notation i_1 in the superscribe of θ^{k,i_1} means that this hypothesis is the most probable extension of $\theta^{k-1,i}$. The best extension corresponds to the hypothesis having maximum marginal likelihood.

To generate the q-best joint hypotheses up to current time step k, firstly each hypothesis $\theta^{k-1,i}$ generates its best extension according to eqns. (15) and (16). These new joint hypotheses are ordered according to their probabilities and stored in the ordered list HYP-LIST. Their probabilities are calculated according to eqn. (14) and stored in PROB-LIST.

Secondly, for each hypothesis in HYP-LIST, use its parent hypothesis to generate the j-th ($j = 2, 3, \cdots$) best extension. If the probability of this extension is higher than the lowest probability in PROB-LIST, add it to HYP-LIST and the corresponding probability to PROB-LIST, and delete the hypothesis with lowest probability from HYP-LIST and its corresponding probability from PROB-LIST. If the probability of this extension is lower than the lowest probability in PROB-LIST, stop generating new extensions by its parent hypothesis. After these processes, we finally obtain the q-best hypotheses up to current time step. The algorithm is described in Tab. 1.

Table 1. q-best hypotheses algorithm

Input: q-best hypotheses up to former time step $\{\theta^{k-1,i}\}_{i=1}^q$ and their corresponding probabilities $\{\beta^{k-1,i}\}_{i=1}^q$ current measurement set $Z(k)$
Output: q-best hypotheses up to current time step $\{\theta^{k,i}\}_{i=1}^q$ and their corresponding probabilities $\{\beta^{k,i}\}_{i=1}^q$
1. Initialize HYP-LIST and PROB-LIST HYP-LIST$\triangleq \{\theta^{k,i_1}\}_{i=1}^q$ $\theta^{k,i_1} \triangleq \{\theta_{i,1}(k), \theta^{k-1,i}\}$ $\theta_{i,1}(k) = \arg\max_{\theta(k)} p(\theta(k) \mid Z^k, \theta^{k-1,s}, U^{k-1})$
2. Order the hypotheses in HYP-LIST according to their probabilities
3. for $i = 1 : q$ If the j-th best new hypothesis generated by $\theta^{k-1,i}$ is still in HYP-LIST, then generate its $(j+1)$-th best new hypothesis. If the probability of the new hypothesis is higher than the lowest probability in PROB-LIST, then add it into the list and delete the hypothesis with the lowest probability. If not, break.
end

4. RESULTS

The rover's position in the navigation frame is represented by the vector (n, e, d) of north, east and down coordinates. In the simulation, we assume that the rover moves in a 2-D plane where $d = 0$. In this case its position and pose can be fully described by the state vector (n, e, ψ) where ψ is the rover's yaw angle. Encoders attached to each rear wheel measure the wheel rotation, which allows computation of the rover speed u and angular rate w.

For the simulated experiment, the vehicle is moving forward with velocity $u = 1m/s$ and a yaw angle of 0^o in the vicinity of the origin. In Fig. 2, the green and blue lines represent the prior estimate and true value of the state trajectory during the first second, respectively. The estimated state trajectory is computed based on the prior knowledge of $x(0)$ and the systems inputs U^K. The trajectory estimate in Fig. 2 is not updated by any photo-detector measurement during its time interval. The encoder and photo-detector work at 1KHz and 10Hz rates, respectively. The green asterisks $*$ in the figure represent the times when a photo-detector measurement occurs. The red line in Fig. 2 represents three times the standard deviation of the state error. Since the encoder measurements cannot perfectly reproduce the rover speed and angular rate, the state error covariance of the prior state grows with time. The length of LED ID recovery circle is $1s$, so there are total of 11 photo-detector time steps.

The following results show the LED ID recovery by a camera. The LED is located at $(2.797, -1.500, -1.500)m$.

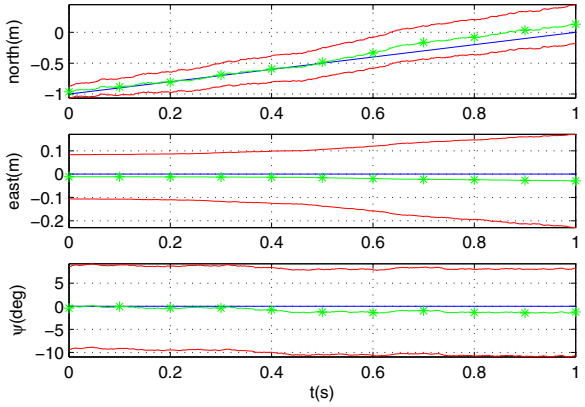

Fig. 2. Navigation state information: Ground truth (blue), Prior trajectory (green), and 3-σ error regions (red)

Fig. 3 shows the camera measurements versus time. The green asterisks represent the a priori prediction of the LED projection location, based on the prior state trajectory estimate. The red line represents three times the standard deviation of the measurement error. Each blue dot is a clutter measurement that falls into the uncertainty ellipse (predicted region), and the magenta dot is the true LED measurement. From the figure, the LED's on-off sequence is $\{1, 1, 0, 0, 1, 1, 0, 0, 1, 1, 0\}$. Fig. 4 shows the uncertainty ellipse and measurements in the two images that are sampled at time 0 and 0.7s, respectively. The figure shows that the predicted LED projection location errors along the two directions are correlated.

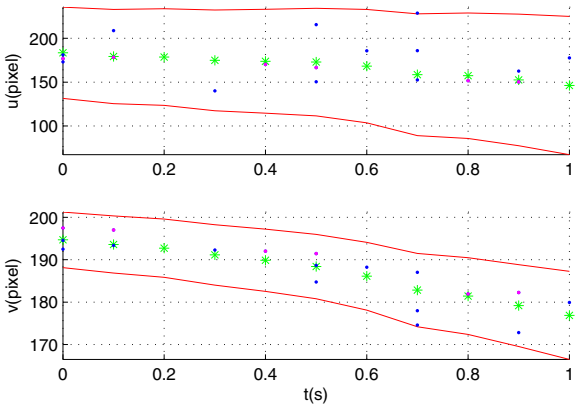

Fig. 3. Camera measurements: Predicted position (green asterisk), Clutter or noise measurement (blue dot), LED measurement (magenta dot), and $3-\sigma$ error regions (red line)

At each measurement time, the detected potential LED projection locations that fall into the uncertainty ellipse are enumerated and stored in the measurement set. The upper left image of Fig. 5 shows the measurements and the prior uncertainty ellipse at time $k = 0$. Since there are three measurements in the ellipse, four data association hypotheses can be generated. Using each data association hypothesis to update the state estimate and then repredict the LED projection location based on each of them, the results are shown in the upper right image of Fig. 5. The ma-

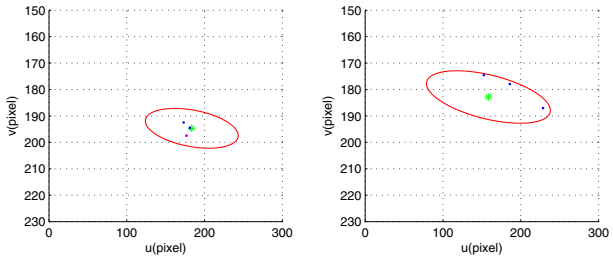

Fig. 4. Camera image plane measurements at time 0 (left) and $0.7s$ (right)

genta "+" symbol represents the predicted LED projection location after updating the state by a hypothesis, and the corresponding magenta ellipse represents its uncertainty. The bottom right image of Fig. 5 shows the predicted LED projection locations at the second measurement time $t = 0.1s$ corresponding to the four hypotheses. At the second measurement step, two potential LED projection locations are measured, which indicates there will be total of 12 hypotheses up to this step. Only the 5 most probable hypotheses are kept and shown in the bottom left image.

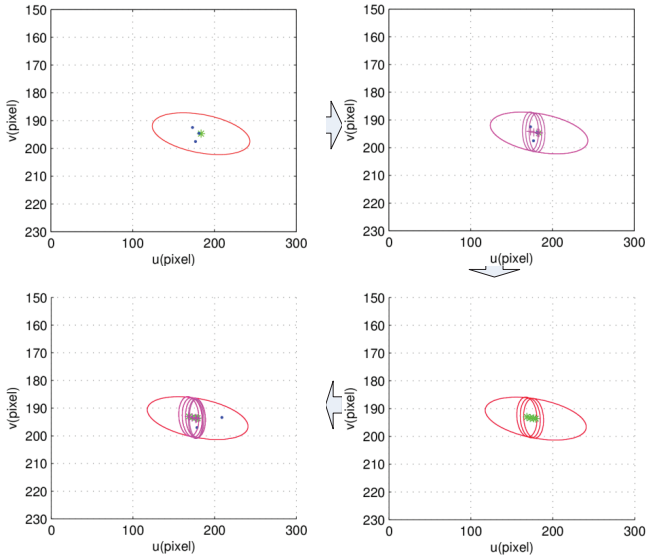

Fig. 5. The process of the algorithm in the first two steps

At $t = 1$, the best 5 hypotheses sequences returned by the algorithm are:

$$\{0, 1, 0, 0, 1, 1, 0, 0, 1, 1, 0\}, \quad \text{with} \quad p = 0.74,$$
$$\{1, 1, 0, 0, 1, 1, 0, 0, 1, 1, 0\}, \quad \text{with} \quad p = 0.12,$$
$$\{3, 0, 0, 0, 1, 1, 0, 0, 1, 1, 0\}, \quad \text{with} \quad p = 0.06,$$
$$\{3, 1, 0, 0, 1, 0, 0, 0, 1, 1, 0\}, \quad \text{with} \quad p = 0.04,$$
$$\{3, 1, 0, 0, 1, 1, 0, 0, 1, 0, 0\}, \quad \text{with} \quad p = 0.04,$$

where 0 represents null, 1 represents the LED detection, and any value greater than 1 represents an erroneous noise or clutter detection. Therefore, the true data association *hypothesis sequence* is $\{1, 1, 0, 0, 1, 1, 0, 0, 1, 1, 0\}$, which is the second best hypothesis with a probability 0.12. Even though it is not the top candidate, the fact that it is always amongst the top candidates, yields reliable data extraction, once the ID and checksum are checked.

Fig. 6 shows a histogram of the position error norm (top) and absolute yaw error (bottom) for the prior and posterior estimates from a simulated experiment with the vehicle in motion. The histogram includes 1000 samples.

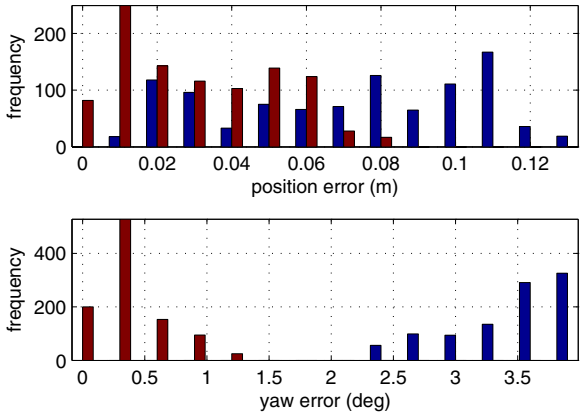

Fig. 6. Prior state estimate error (blue) and posterior state estimate error (red)

5. CONCLUSION AND FUTURE WORK

This paper has developed and presented an LED path recovery algorithm that is applicable to either a camera and linear array, whether the photo-detector is moving or stationary. This algorithm has utility in VLC applications, particularly with the problem of accurately and reliably extracting a data sequence communicated by an LED to a camera or linear array. This approach is based on the MHT. The presentation included analysis and discussion of the hypothesis probability model and measurement model. This article has focused on processing of a single LED. The situation when a measurement can fall into multiple LEDs' uncertainty ellipse is not considered. Future work will consider the approach that associates the measurements to multiple LEDs' jointly.

When multiple LED's data association are jointly considered, each LED's data association hypothesis at a time step not only depends on its own former association hypotheses, but also other LEDs' association hypotheses. This could greatly increase the complexity of the assignment of the measurements to the LED's. This could be addressed by efficient assignment algorithms such as Auction Bertsekas (1988) and JVC algorithm Jonker and Volgenant (1987). Finally, on-robot in-lab testing and demonstration of these methods are underway.

ACKNOWLEDGEMENTS

This project was supported by the Ubiquitous Communication by Light (UC-Light) Center. The project is part of the University of California (UC) Multicampus Research Program and Initiatives (MRPI) under grant 142787.

REFERENCES

Arai, S., Mase, S., Yamazato, T., Yendo, T., Fujii, T., Tanimoto, M., and Kimur, Y. (2008). Feasible study of road-to-vehicle communication system using LED array and high-speed camera. *15th World Congress on IT*.

Bar-Shalom, Y., Blackman, S.S., and Fitzgerald, R.J. (2005). The dimensionless score function for multiple hypothesis decision in tracking. In *IEEE Int. Conf. SMC*.

Bar-Shalom, Y., Daum, F., and Huang, J. (2009). The probabilistic data association filter. *IEEE CSM*, 29(6), 82–100.

Bertsekas, D.P. (1988). The auction algorithm: A distributed relaxation method for the assignment problem. *Annals of operations research*.

Cox, I.J. and Hingorani, S.L. (1996). An efficient implementation of reid's multiple hypothesis tracking algorithm and its evaluation for the purpose of visual tracking. *IEEE PAMI*, 18(2), 138–150.

Elfring, J., Janssen, R., and Molengraft, R.v.d. (2010). Data association and tracking: A literature survey. Technical report, RoboEarth.

Farrell, J.A. (2008). *Aided Navigation: GPS with High Rate Sensors*. McGraw-Hill.

Frank, A., Smyth, P., and Ihler, A. (2012). A graphical model representation of the track-oriented multiple hypothesis tracker. In *IEEE SSPWF*, 768–771.

Jonker, R. and Volgenant, A. (1987). A shortest augmenting path algorithm for dense and sparse linear assignment problems. *Computing*.

Kavehrad, M. (2007). Broadband room service by light. *Scientific American*.

Kurien, T. (1990). Issues in the design of practical multitarget tracking algorithms. *Multitarget-Multisensor Tracking: Adv. Appl.*

Liu, J., Noonpakdee, W., Takano, H., and Shimamoto, S. (2011). Foundational analysis of spatial optical wireless communication utilizing image sensor. In *IEEE Int. Conf. Imaging Syst. and Tech.*

Maesschalck, D., Jouan-Rimbaud, D., and Massart, D. (2000). The Mahalanobis distance. *Chemometrics and Intelligent Laboratory Systems*, 50.

Murty, K.G. (1968). An algorithm for ranking all the assignments in order of increasing cost. *Operations Res.*, 16, 682–687.

Nagura, T., Yamazato, T., Katayama, M., Yendo, T., Fujii, T., and Okada, H. (2010). Improved decoding methods of visible light communication system for ITS using LED array and high-speed camera. In *IEEE Veh. Tech. Conf.*

Reid, D. (1979). An algorithm for tracking multiple targets. *IEEE TAC*, 24(6), 843–854.

Robert, R. (2013). Intel labs camera communications (CamCom). Technical report, Intel Lab.

Zheng, D., Chen, G., and Farrell, J.A. (2013a). Navigation using linear photo-detector arrays. In *IEEE MSC*.

Zheng, D., Chen, G., and Farrell, J.A. (2014). An algorithm to recover an LED path. In *ECC, Accepted*.

Zheng, D., Cui, K., Bai, B., Chen, G., and Farrell, J.A. (2011). Indoor localization based on LEDs. In *IEEE MSC*, 573–578.

Zheng, D., Vanitsthian, R., Chen, G., and Farrell, J.A. (2013b). LED-based initialization and navigation. In *ACC*, 6199–6205.